論文 / 著書情報
Article / Book Information

Title	Research on Electric Current Control of Power Generation Using Droplet Network
Author	Shuji Kikuchi, Shoichiro Kanno, Kenta Shimba, Yoshitaka Miyamoto, Tohru Yagi
Journal/Book name	2025 17th Biomedical Engineering International Conference (BMEiCON), , ,
Pub. date	2025, 7
DOI	https://doi.org/10.1109/BMEiCON66226.2025.11113716
Copyright	(c)2025 IEEE. Personal use of this material is permitted. Permission from IEEE must be obtained for all other uses, in any current or future media, including reprinting/republishing this material for advertising or promotional purposes, creating new collective works, for resale or redistribution to servers or lists, or reuse of any copyrighted component of this work in other works.
Note	This file is author (final) version.

Research on Electric Current Control of Power Generation Using Droplet Network

Shuji Kikuchi
Dept. of Mechanical Engineering
Inst. of Sci. Tokyo
Tokyo, Japan
kikuchi.s.af7f@m.isct.ac.jp

Shoichiro Kanno
Dept. of Mechanical Engineering
Inst. of Sci. Tokyo
Tokyo, Japan
kanno.s.ad@m.titech.ac.jp

Kenta Shimba
Graduate Sch. of Frontier Sci.
The Univ. of Tokyo
Chiba, Japan
shimba@neuron.t.u-tokyo.ac.jp

Yoshitaka Miyamoto
National Research Inst.
for Child Health and Development
Tokyo, Japan
myoshi1230@gmail.com

Tohru Yagi
Dept. of Mechanical Engineering
Inst. of Science Tokyo
Tokyo, Japan
yagi.t.ab@m.titech.ac.jp

***Abstract*— A method has been proposed to create batteries with properties suitable for bio-induction using droplet networks that mimic the power-generating organs of electric fish. In this study, we attempt to develop current output control using a droplet network battery. The minimum droplet network battery has been fabricated and utilized for power generation, indicating that the current output can be controlled by adjusting the membrane area. It is also suggested that the output at the start of power generation and the α-HL insertion rate can be successfully improved by adding an external constant voltage during battery fabrication.**

***Index Terms*— Biological devices, Droplet network, Membrane protein, Power generation, Current control.**

I. Introduction

Bio-embedded devices require a power source that is flexible, biocompatible, and capable of generating and using materials in living organisms. A battery that mimics the power-generating organ of an electric fish has been proposed as a power source that meets these requirements [7]. In the electric eel's power-generating organ, the inflow and outflow of ions are controlled by membrane proteins that connect the inside and outside of the cell, generating a potential difference. Methods to reproduce this mechanism using droplet networks have been studied [3]. Lipid bilayers formed at the contact zone of droplets in lipid solutions exhibit properties similar to those of biological cell membranes. Chemical gradient batteries can be fabricated by linking droplets with different ion concentrations and inserting membrane proteins into the lipid bilayer membrane (Figure 1). Although power generation with such droplet network batteries has been successful, challenges remain related to output control and initial output stability.

The current output of the battery increases in proportion to the rate of membrane protein insertion. The maximum insertion rate of membrane proteins can be increased by increasing the area of the lipid bilayer. Additionally, by creating a potential difference between droplets, a pore is formed in the lipid bilayer membrane, thereby increasing the insertion probability of membrane proteins [6]. The output during power generation can be controlled by applying an external force to the droplet to change the membrane area. Additionally, by applying a constant voltage externally before the start of power generation, membrane proteins can be inserted in advance, thereby improving the initial output. Based on the above hypothesis, experiments were conducted to control the output during power generation by applying external loading and to enhance the output at the start of power generation by applying a constant external voltage.

II. Experimental Methods

A. Fabrication of Droplet Network Battery

Ag/AgCl electrodes were prepared by applying AgCl paste to the tips of two Ag wires 0.20 mm in diameter and drying overnight. Each electrode was fixed to a micromanipulator and connected to the electrical measurement device. Agarose gel (10 mM HEPES, 1% agarose) and aqueous solution (10 mM HEPES) containing 0.05 μg/mL α-hemolysin (α-HL) were prepared as components of the droplets. Two solutions and gels were prepared with a KCl concentration ratio of 0.5 M : 1.5 M. 1 μL of agarose gel was applied to the tip of each electrode, and 0.8 μL of the solution was dropped. 300 μL of phospholipid hexadecane (10 mM DPhPC) was prepared and poured into an acrylic chamber. To form a lipid monolayer on the droplet surface, the droplet at the electrode tip was immersed in the hexadecane solution and left for 30 min. The minimum droplet network battery was the one that connected the two droplets.

B. Power generation and output control

Figure 2 shows the power generation using a droplet network battery. K^+ moves along an ionic gradient through α-HL inserted in the lipid bilayer between the droplets, causing a redox

979-8-3315-1444-0/25/$31.00 ©2025 IEEE

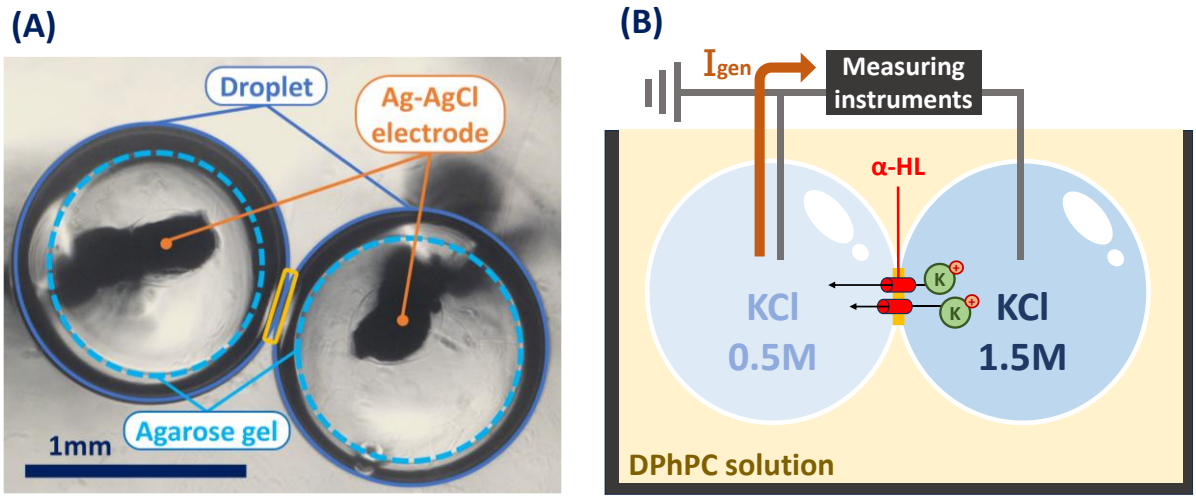

Fig. 1. Droplet network battery. (A) Microscopic photo observed from below the chamber. (B) Schematic diagram of the power generation mechanism.

reaction on each electrode to generate electricity. Two droplets were connected, and the current output was recorded until it began to rise and then slowly declined. For measuring electrical properties and applying external voltage, a patch clamp amplifier (AxoPatch 200B, Molecular Devices), an AD converter (PowerLab 4/15T, ADInstrument), and a function generator (FG-281, KENWOOD) were used.

The current output was then controlled by external force loading. After approximately 500 seconds had elapsed since the current output began to drop, the micromanipulator was manipulated to apply an external force between droplets via the electrodes. The relationship between the contact area and the resulting change in current output was recorded. The film area before and after external force loading is estimated from the photographed images of the droplets. The contact surface is assumed to be a circle, and the contact length is calculated as the diameter.

C. Improvement of characteristics by external voltage

After connecting the newly fabricated droplet, a steady voltage of 50 mV was applied in the opposite direction of the droplet's ionic gradient. At this time, the ion concentration change in the droplet is considered to stop. The droplet was allowed to stand until the current became sufficiently large in the negative direction. The current response was recorded during a series of operations, and the external constant voltage was stopped to initiate forward power generation. The current response during the series of operations was recorded to evaluate the effect of the external constant voltage on the output at the start of power generation and the insertion rate of α-HL.

III. Analysis Method

The increase in conductance due to a single α-HL insertion is approximately 775 pS [1]. This value was used to compare the

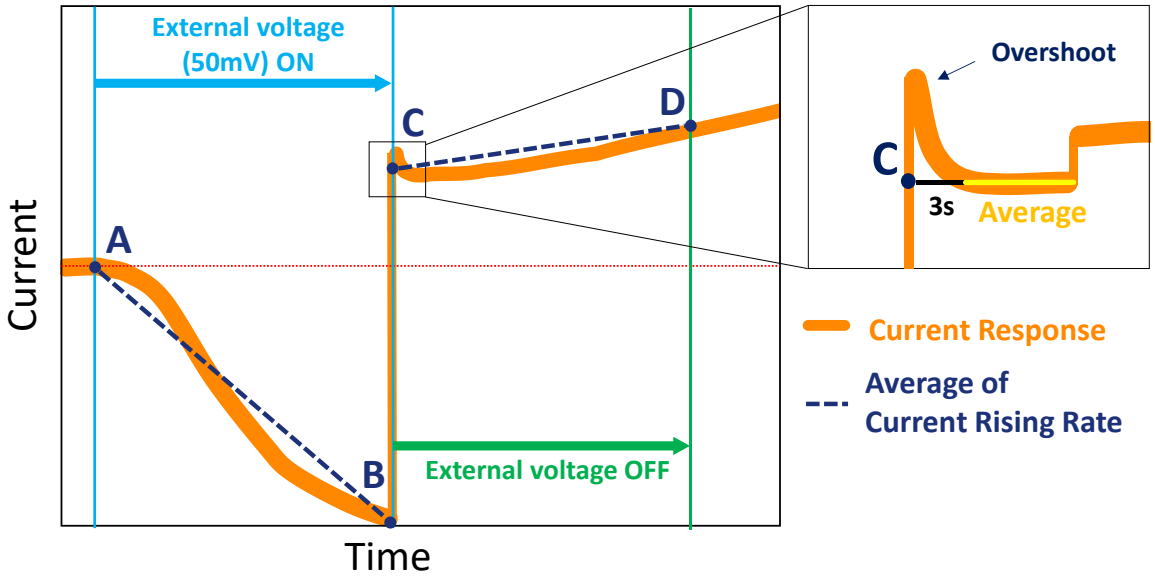

Fig. 2. Schematic diagram illustrating the current response upon application of external voltage and subsequent power generation.

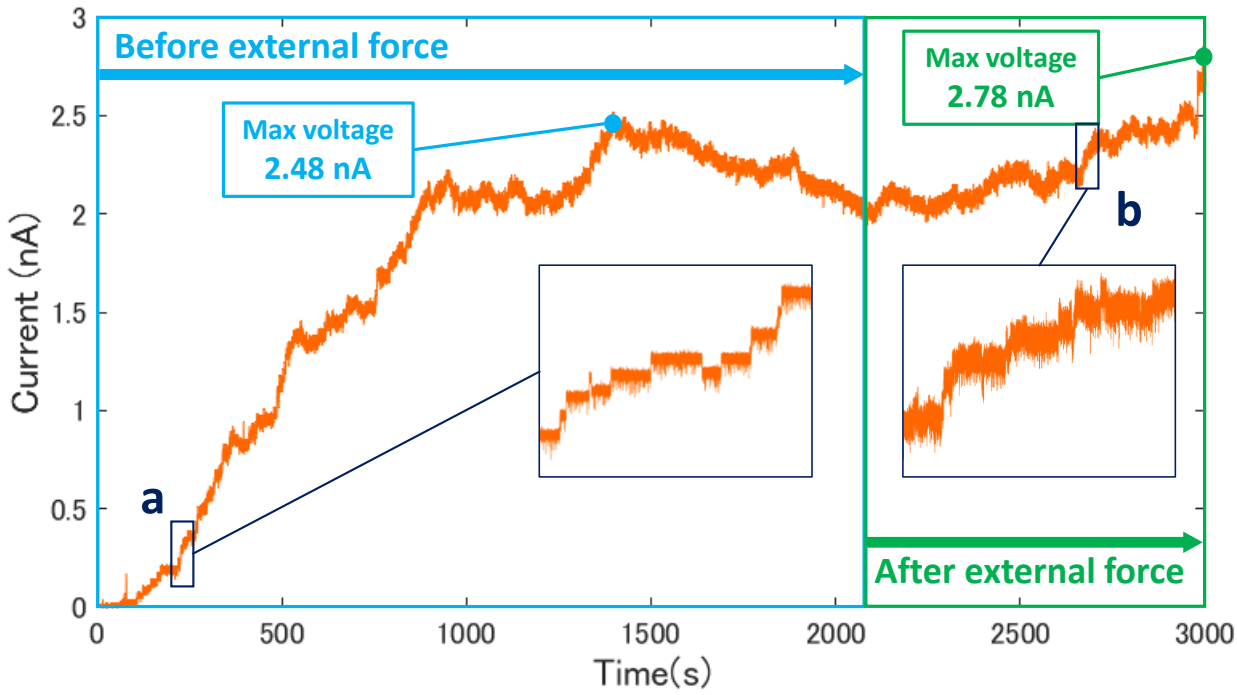

Fig. 3. The current response recorded during a series of operations, along with the dilation waveforms at (a) and (b).

Table 1. Comparison of change in maximum current output and droplet contact area.

	Before	After	Leverage
Maximum current [nA]	2.48	2.78	× 1.12
contact area [mm^2]	0.056	0.066	× 1.18

α-HL insertion rate per hour during external constant voltage application and power generation. Figure 4 shows a schematic of the current response during external voltage application and subsequent power generation. The insertion amount Ins_{AB}, Ins_{CD} of α-HL per time t in the intervals AB and CD were defined as follows in Equations 1 and 2.

$$Ins_{AB} = (I_B - I_A) / (775 \times 10^{-12} \times V_{AB} \times t) \quad (1)$$

$$Ins_{CD} = (I_D - I_C) / (775 \times 10^{-12} \times V_{CD} \times t) \quad (2)$$

For the currents at each time point used in the calculations, we used 0 nA for I_A, the average value during the 0.5 s period just before switching for I_B, and the average value during the 0.5 s period before and after switching for I_D. For I_C, to exclude any overshoot originating from the recording device, the average value from 3 s after the voltage switch to the next α- HL insertion. Additionally, the uppercase I with a subscript C was used for the output at the start of power generation. For each section of voltage, V_{AB} used a magnitude of the external constant voltage of 50 mV, and V_{CD} was expressed in terms of the values of I_B and I_C as in the following Equation 3.

$$V_{CD} = (I_C / I_B) \times V_{AB} \quad (3)$$

IV. Results and Discussion

A. Power generation and output control

Figure 3 shows the current response recorded during a series of operations and the dilation waveforms at 220-280 s (a) and 2660-2720 s (b). The light blue and green boxes represent the before and after membrane area adjustments by external force loading, respectively. Table 1 presents the change in maximum current output before and after the application of an external force, as well as the change in film area estimated from the droplet images. Current waveforms with stepwise increases were observed both before and after external loading. These waveforms are attributed to the insertion of α-HL into the lipid bilayer over time, resulting in a stepwise increase in conductance between droplets [3]. This suggests that the insertion of new α-HL reached its maximum amount at about 1400 s, stopped, and then resumed when the membrane area expanded due to the external force. The rates of change in maximum current output and film area were close together at 0.06 points, suggesting a proportional relationship between the two. This error can be attributed mainly to the low accuracy of the image analysis method. For more accurate film area evaluation, further improvement of image analysis accuracy is needed, for example, by capturing images from different angles.

B. Improvement of characteristics by external voltage

Figure 4 shows the current responses obtained in two trials, which are Data 1 and Data 2, respectively. Table 2 shows the amplitude of the expanded current waveform, external steady-state voltage application time, output at the start of power generation, and α-HL insertion rate before and after voltage switching, calculated from the measured current responses.

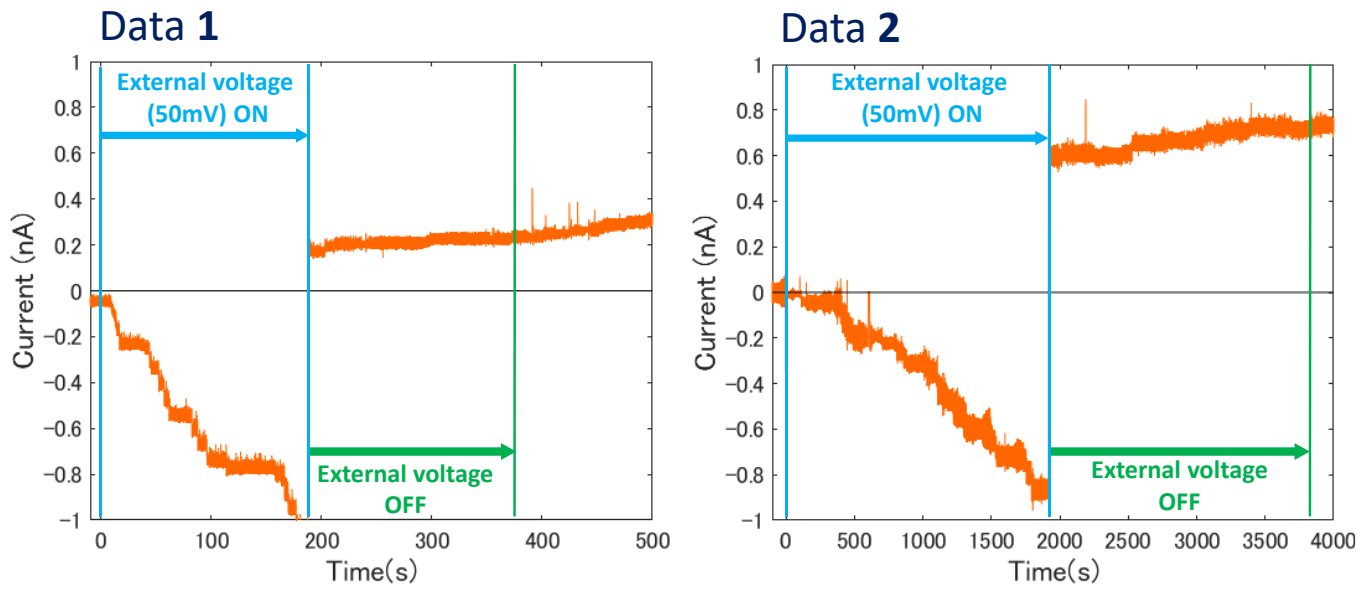

Fig. 4. The current response at Data 1 and 2.

Table 2. Comparison of each data of Data 1 and 2.

Data	amplitude $[nA]$	Time $[s]$	Output at start $[nA]$	Ins_{AB} $[s^{-1}]$	Ins_{CD} $[s^{-1}]$
	$\times 10^{-2}$			$\times 10^{-3}$	$\times 10^{-3}$
1	1.12	220	0.175	117	48.5
2	4.76	1942	0.595	11.5	3.37

The α-HL insertion was accelerated by the application of external constant voltage before the start of power generation, and positive power output was obtained from the start of power generation, as hypothesized. The fact that $Ins_{AB} > Ins_{CD}$ is valid for both data suggests that the insertion of α-HL was accelerated by the application of external constant voltage, and the time required for the battery output to increase was shortened.

However, the insertion rate may decrease as the α-HL insertion approaches its maximum value. For accurate evaluation, it is necessary to apply voltage to the data for a short time, ensuring that the amount of α-HL insertion does not reach its maximum value.

V. Conclusion

A minimal droplet network battery was fabricated and utilized to generate electricity, indicating that the current output could be controlled by altering the film area. The results also suggest that the addition of an external constant voltage during battery fabrication successfully increased the output at the start of power generation and the α-HL insertion rate. In the future, we plan to develop methods to evaluate the relationship between battery output and film area more accurately. Additionally, we aim to enhance the output by increasing the number of connected droplets, improving energy efficiency and mechanical strength by modifying the material, and introducing new functions.

Acknowledgment

This work was supported by JSPS KAKENHI (Grant Nos. JP23K25191, JP23KJ0925).

References

[1] G. Miles, S. Cheley, O. Braha, and H. Bayley, “The Staphylococcal Leukocidin Bicomponent Toxin Forms Large Ionic Channels,” Biochemistry, vol. 40, no. 29, pp. 8514–8522, 2001.

[2] J. El-beyrouthy and E. Freeman, “Characterizing the Structure and Interactions of Model Lipid Membranes Using Electrophysiology”, Membranes., vol. 11, No.5, p.319, 2021.

[3] K. Hongo, Z. Peng, K. Shimba, Y. Miyamoto, and T. Yagi, "Development of a Battery Using a Hydrogel Network," 2022 14th BMEiCON, pp. 1–4, 2022.

[4] L. C. M. Gross, A. J. Heron, S. C. Baca, and M. I. Wallace, “Determining membrane capacitance by dynamic control of droplet interface bilayer area,” Langmuir, vol. 27, no. 23, pp. 14335–14342, 2011.

[5] M. Naumowicz and A. D. Petelska, “Capacitance and resistance of the bilayer lipid membrane formed of phosphatidylcholine and cholesterol,” Cell Mol Biol Lett., vol. 8, no. 1, pp. 5–18, 2015.

[6] S. Renner, A. Bessonov, and F. C. Simmel, “Voltage-controlled insertion of single α-HL and Mycobacterium smegmatis nanopores into lipid bilayer membranes smegmatis nanopores into lipid bilayer membranes”, Appl. Phys. Lett., vol. 98, No.8, pp.1–4, 2011.

[7] Thomas B. H. Schroeder, Anirvan Guha, Aaron Lamoureux, Gloria Van Renterghem, David Sept, Max Shtein, Jerry Yang, and Michael Mayer, “An electric-eel-inspired soft power source from stacked hydrogels”, Nature, vol.552, pp.214–218, 2017.